Specific interaction between Group B *Streptococcus* CC17 hypervirulent clone and phagocytes

Anne-Sophie Bourrel[1,2,×], Amandine Picart[1,×], Jose-Carlos Fernandez[1], Constantin Hays[1,2], Virginie Mignon[4], Bruno Saubaméa[4], Claire Poyart[1,2,3], Agnès Fouet[1], Asmaa Tazi[1,2,3], Julie Guignot[1*]

[1]Université Paris Cité, Institut Cochin, INSERM, U1016, CNRS, UMR8104, F-75014 Paris, France; [2]Hôpitaux Universitaires Paris Centre, Cochin, Assistance Publique Hôpitaux de Paris, France; [3]Centre National de Référence des Streptocoques, France ; [4]Plateforme PICMO, US25 INSERM, UAR3612 CNRS, Faculté de Pharmacie, Université Paris Cité, Paris, France.

[×] These authors contributed equally to this work

***** To whom correspondence should be addressed: julie.guignot@inserm.fr

ORCID number: 0000-0001-8890-4028. Tel: + 33 1 40 51 64 13; Fax: + 33 1 40 51 64 54.

Institut Cochin, 22 rue Méchain 75014 Paris, France.

ORCID number A. Fouet, 0000-0001-7715-9157;

CONFLICT OF INTEREST:

The authors have declared that no conflict of interest exists.

Keywords: CC17, *Streptococcus agalactiae*, Group B *Streptococcus*, phagocytosis, adhesion, THP-1.

Running title: Hypervirulent Group B Streptococcus and phagocytes

Abbreviations: CC17 (clonal complex 17), GBS (group B *Streptococcus*).

ABSTRACT

Streptococcus agalactiae also named Group B *Streptococcus* (GBS) is the most significant pathogen causing invasive infections, such as bacteremia and meningitis, in neonates. Worldwide epidemiological studies have shown that a particular clonal complex (CC) of capsular serotype III, the CC17, is strongly associated with meningitis in neonates and is therefore designated as the hypervirulent clone. Macrophages are a permissive niche for intracellular bacteria of all GBS clones. In this study we deciphered the specific interaction of GBS CC17 strains with macrophages. Our study revealed that CC17 strains are phagocytosed at a higher rate than GBS non-CC17 strains by human monocytes and macrophages both in cellular models and primary cells. CC17 enhanced phagocytosis is due to an initial enhanced-attachment step to macrophages mediated by the CC17 specific surface protein HvgA and the PI-2b pilus (Spb1). We showed that two different inhibitors of scavenger receptors (fucoidan and poly(I)) specifically inhibited CC17 adhesion and phagocytosis while not affecting those of non-CC17 strains. Once phagocytosed, both CC17 and non-CC17 strains remained in a LAMP-1 positive vacuole that ultimately fuses with lysosomes where they can survive at similar rates. Finally, both strains displayed a basal egress which occurs independently from actin and microtubule networks. Our findings provide new insights into the interplay between the hypervirulent GBS CC17 and major players of the host's innate immune response. This enhanced adhesion leading to higher phagocytosis could reflect a peculiar capacity of the CC17 lineage to subvert the host immune defenses, establish a niche for persistence or disseminate.

41 **INTRODUCTION**

42 The innate immune system plays a crucial role during host's interaction with pathogens, particularly in
43 neonates who exhibit a naive adaptive immune system and are more vulnerable to invasive infections
44 (1). Innate immunity largely relies on professional phagocytic cells, which constitute the first line of
45 defense against pathogens. The large repertoire of phagocytic surface receptors that mediate the
46 binding and internalisation of the pathogen is divided in opsonic and non-opsonic receptors. Opsonic
47 receptors include the Fc receptors and complement receptors, which recognize antibody- or
48 complement-opsonized pathogens, but also some non-opsonized pathogens (2, 3). Non-opsonic
49 receptors are constituted by a wide array of family receptors including Toll like receptors (TLRs),
50 integrins, C-type lectins or scavenger receptors that directly interact with pathogen-associated
51 molecular patterns (PAMPs). Receptor recognition triggers intracellular signaling cascades leading to
52 actin polymerization- which generates membrane protrusions required for bacterial engulfment.
53 Signal transduction during phagocytosis is specific to the cell type and to the receptor(s) involved and
54 can impact the intracellular fate of the microorganism (4). Once internalized, the pathogen resides in
55 a phagosome, which rapidly undergoes maturation and acquires numerous proteins such as the late
56 endosome/lysosome-associated membrane proteins LAMP-1 and LAMP-2. Ultimately, the phagosome
57 fuses with lysosomes to become a phagolysosome with microbicidal features including a very acidic
58 lumen (pH ~ 4.5), lysosomal proteases, and reactive oxygen species (ROS). This in turn leads to
59 microbial killing and production of pro-inflammatory mediators that orchestrate the initiation of
60 adaptive immunity.

61 *Streptococcus agalactiae*, also named Group B *Streptococcus* (GBS), is a capsulated chain-forming
62 Gram-positive coccus commonly found in the gut and the lower urogenital tract of approximately 20%
63 healthy adults (5). Although rarely pathogenic in adults, GBS is the leading cause of invasive infections
64 in neonates (6). Two neonatal GBS-associated syndromes, referred to as "early-onset disease" (EOD)
65 and "late-onset disease" (LOD), have been described, depending on the age at onset. EOD often
66 manifests by respiratory distress that rapidly progresses into bacteremia and less frequently
67 meningitis. In contrast, LOD manifests as a bacteremia highly associated with meningitis (20-50%
68 cases) (7, 8). Based on the capsular polysaccharide composition, GBS has been classified into 10 distinct
69 serotypes (Ia, Ib, and II–IX). Serotype III is the most frequently identified serotype in young infants
70 (61.5%) (9). More specifically, within serotype III, multilocus sequence typing (MLST) has identified a
71 hypervirulent lineage termed clonal complex 17 (CC17) which accounts for a substantial proportion
72 (25%) of EOD cases and the vast majority (70%) of LOD cases worldwide, whereas it is isolated in about
73 only 13% of non-pregnancy-related adult infections and colonization (7, 10, 11). GBS CC17 is a highly
74 successful invasive clone in the neonate strongly associated with neonatal meningitis (~70%) in both

75 EOD and LOD (12-14). CC17 strains harbor a number of specific genes including the genes encoding
76 two surface proteins named Srr2 and HvgA that are involved in the crossing of the intestinal and blood
77 brain barriers (8, 15-17). Although not totally exclusive to the CC17 lineage, the pilus island PI-2b
78 encoding the Spb1 adhesin is found in the vast majority of the CC17 strains, while rarely present in
79 other human lineages (15, 18).

80 GBS has developed several mechanisms to resist immune detection, phagocytosis and microbial
81 degradation (19). The capsular polysaccharide (CPS) is one of the major virulence factors of GBS
82 allowing evasion from the host immune system, notably by preventing host complement deposition
83 on the bacterial surface (20, 21). Although capsule limits phagocytosis of complement-opsonized GBS,
84 opsonized-GBS can be phagocytosed by Fc and complement receptors respectively (19, 22). However,
85 there are large gaps in our understanding of the phagocytosis of non-opsonized GBS. The receptor(s)
86 and signaling pathway(s) involved in non-opsonized GBS phagocytosis are unknown. Interestingly, non-
87 opsonized GBS uptake leads to a better survival within phagocytes (19, 23-25). The persistence of GBS
88 in macrophages relies on numerous bacterial factors (19, 26). The expression of some virulence factors
89 associated to the CC17 lineage such as Spb1 have been described to increase phagocytosis (27-29).
90 However, the capacity of the CC17 lineage to exhibit enhanced phagocytosis and survival in
91 macrophages compared to those of other GBS lineages is still disputed (25, 30-32).

92 In the present study, we used a collection of GBS isolates representing a range of capsular types and
93 CCs and showed that CC17 strains are more phagocytosed than non-CC17 isolates. Our data support
94 that the enhanced phagocytosis of CC17 strains is solely due to an increased initial adhesion to
95 phagocytes. Once internalized, GBS CC17 and non-CC17 do not differentially affect the phagolysosome
96 maturation nor their ability to survive within phagocytes and can be released in the extracellular
97 compartement.

98

99 **RESULTS**

100 **GBS CC17 strains are more phagocytosed than non-CC17 strains by macrophages and monocytes**

101 The literature shows conflicting results on GBS lineages capacity to be phagocytosed (25, 30-32).
102 Therefore, we performed a phagocytosis assay using THP-1 differentiated macrophages to compare
103 the level of phagocytosis of a relevant collection of GBS isolates responsible for human invasive
104 infections including 27 CC17 strains and 40 non–CC17 strains (Table S2, Fig. 1A). The CC17 strains were
105 more phagocytosed than the non-CC17 strains (2.3-fold increase). To further characterize the lineage
106 differences and the phagocytosis process, we next used two well-characterized and fully sequenced
107 GBS isolates, one CC17 strain (BM110) and one CC23 strain (NEM316). They displayed a difference in
108 phagocytosis level comparable to that of CC17 versus non-CC17 strains in THP-1 macrophages (2.5-
109 fold increase) (Fig. S1). Using these two strains, we confirmed the higher phagocytosis of GBS CC17 in
110 primary human monocytes derived macrophages (hMDM) (Fig. 1B), in non-differentiated THP-1
111 monocytes (Fig. 1C) and in primary human monocytes (Fig. 1D).
112 Since the capsule is a major bacterial factor involved in GBS phagocytosis, we analyzed its contribution
113 to the enhanced phagocytosis of GBS CC17 strains. First, we stratified the results of the phagocytosis
114 assay performed with the clinical GBS strains presented in Fig. 1A according to their capsular type.
115 CC17 strains being almost exclusively of capsular type III and more rarely of type IV, we distinguished
116 within CC17 and non-CC17 isolates those of capsular type III, IV and all the other types (Fig. 2A). The
117 CC17 strains higher phagocytosis was independent from the capsular type. To further test the influence
118 of the capsular type, we analyzed the phagocytosis level of BM110 and NEM316 mutants, inactivated
119 for capsule expression. As expected, an increased phagocytosis of the capsule deficient strains was
120 observed with both mutant strains (Fig. 2B). Furthermore, the higher phagocytosis of the CC17 isolate
121 compared to the non-CC17 isolate could also be observed with the corresponding non-capsulated
122 mutants (Fig. 2B).
123 Altogether, these results show that CC17 strains are more phagocytosed than non-CC17 strains in a
124 capsule independent manner.

125 **HvgA and Spb1 promote phagocytosis of CC17 strains**

126 This observation prompted us to search for CC17 specific virulence factors that may account for this
127 enhanced phagocytosis. To this end, we tested the phagocytosis level of BM110 inactivated in genes
128 encoding CC17-specific (Srr2, HvgA) or -highly associated (Spb1) surface proteins (Fig. 3A) (15). Both
129 *ΔhvgA and Δspb1* mutants exhibited reduced phagocytosis in THP-1 macrophages (65% and 54%
130 reduction, respectively) compared to the wild-type (WT) strain. In contrast, there was no difference
131 between the phagocytosis of the Δ*ssr2* and the WT strain. The role of Spb1 in GBS phagocytosis has
132 already been described (27, 28, 33), but not that of HvgA. To confirm the direct involvement of the

133 HvgA surface protein in phagocytosis, we used a close relative non-pathogenic *Lactococcus lactis*, in
134 which an expression vector encoding HvgA and enabling its presentation at the bacterial surface was
135 introduced (16). The heterologous expression of HvgA in *L. lactis* led to a 3-fold increase in
136 phagocytosis, as compared to *L. lactis* carrying an empty vector (Fig. 3B). The involvement of HvgA in
137 CC17 phagocytosis was also observed using hMDM (Fig. 3C).

138 **The signal transduction leading to phagocytosis is similar between CC17 and non-CC17 strains**

139 Cell membrane protrusion formation leading to bacterial engulfment results from cytoskeleton
140 rearrangements, which are mediated by specific signaling cascades induced by bacterial binding to cell
141 surface receptors (34). Numerous signaling molecules regulate the cytoskeleton, including the small
142 Rho GTPases Rho, Rac and CDC42 known to allow the formation of actin stress fibers, lamellipodial
143 protrusions, and filopodia, respectively (35). To better characterize the molecular pathways involved
144 in GBS engulfment, we performed phagocytosis assays using a wide array of inhibitors targeting
145 different signaling molecules (Table S3, Fig. 4A). BM110 phagocytosis was inhibited by cytochalasin D,
146 ZCL278, staurosporine, LY29002 and PP2 indicating that CC17 phagocytosis required actin, the small
147 GTPase CDC42, as well as the different kinases, PKC, Pi3K and Src, respectively. In contrast,
148 microtubules, the small GTPase Rac and the kinases Syk and Rock were not involved in CC17
149 phagocytosis, as indicated by the absence of effect of nocodazole, NSC23766, BAY61-3606 and Y27632
150 respectively (Fig. 4A). Interestingly, we found that NEM316, BM110Δ*hvgA* or BM110Δ*spb1*
151 phagocytosis involved the same signaling proteins than BM110 (Fig. 4B, 4C and 4D respectively).
152 To gain further insight into these findings, we characterized the early contact between GBS and
153 macrophages, which occurs prior to phagocytosis by Scanning Electron Microscopy (SEM) (Fig. 4E).
154 SEM revealed that numerous BM110 chains were adherent to macrophages in contrast to only a few
155 NEM316 chains (Fig. 4E, left panel). In addition, the uptake of both BM110 and NEM316 was
156 accompanied by the formation of filopodia-like cellular protrusions that were observed at 15 min
157 (Fig.4E, middle panel) and lamellipodia-like structure at 30 min (Fig. 4E, right panel).
158 Taken together, our results show that CC17 and non-CC17 are both captured by filopodia and that
159 bacterial uptake involves similar signaling proteins. Our results also suggest that enhanced
160 phagocytosis of CC17 strains may be due, at least in part, to an increased adhesion.

161 **CC17 enhanced phagocytosis is due to initial higher adhesion**

162 To test a potential adhesion difference between CC17 and non-CC17 strains, we analyzed the adhesion
163 of GBS strains to THP-1 macrophage. To prevent bacterial engulfment, adhesion was assessed either
164 at 4°C or at 37°C in the presence of cytochalasin D, an inhibitor of actin polymerization (Fig. S2A). Data
165 showed that bacterial adhesion to phagocytes was similar for all strains independently of the method
166 used to block phagocytosis. In both cases, adhesion of the BM110 strain was higher than that of

167 NEM316. We next assessed adhesion at 4°C and observed a higher adhesion of CC17 clinical strains
168 than of non-CC17 strains (1.9-fold increase, Fig. 5A, Table S2) to THP-1 macrophages. The enhanced
169 adhesion was also observed with strain BM110 compared to NEM316 on THP-1 macrophages (Fig.
170 S2A), THP-1 monocytes (Fig. 5B) and hMDM (Fig. 5C). As observed for phagocytosis, the increased
171 adhesion of CC17 isolates was not related to the capsular serotype (Fig. S2B) and was still observed in
172 the absence of capsule expression (Fig. 5D). Both *ΔhvgA and Δspb1* mutants exhibited reduced
173 adhesion on THP-1 macrophages (23% and 48% reduction, respectively) compared to the WT strain
174 (Fig. 5E). The heterologous expression of HvgA in *L. lactis,* led to a 2-fold increase in adhesion to THP-
175 1 macrophages, relative to *L. lactis* carrying an empty vector (Fig. 5F). The involvement of HvgA in CC17
176 adhesion was also observed using hMDM (Fig. S2C). These results indicate that CC17 strains have a
177 higher level of adhesion compared to non-CC17 strains. Furthermore, the increased adhesion of CC17
178 strains is mediated by both Spb1 and HvgA.

179 To determine whether CC17 higher phagocytosis was solely due to the increased adhesion or to a more
180 complex phenomenon involving both increased adhesion and uptake, we compared the ratio of
181 phagocytosed bacteria to the initial number of adherent bacteria. BM110 and its derivative mutant
182 strains and NEM316 strains showed similar ratios of phagocytosed bacteria (Fig. 5G). Next, we infected
183 THP-1 macrophages with the strain BM110 at a lower multiplicity of infection than NEM316 (MOI 2
184 and MOI 10, respectively) to obtain similar numbers of adherent bacteria (Fig. 5H). In that case, similar
185 numbers of phagocytosed bacteria were obtained with both strains.
186 Taken together, our results show that the enhanced phagocytosis of BM110 strain is solely due to its
187 initial increased adhesion to macrophages.

188 **CC17 uptake by macrophages is inhibited by scavenger receptor inhibitors**

189 Phagocytes express multiple receptors involved in bacterial adhesion and uptake. To identify the
190 precise nature of the macrophage receptor(s) involved in GBS recognition and uptake, GBS CC17
191 phagocytosis was evaluated in cells pre-treated with various blocking molecules targeting putative
192 receptor(s) (Table S3, Fig. 6A). Whereas the inhibitors targeting FCγR, complement receptors, integrins
193 and lectin receptors did not affect GBS CC17 phagocytosis, fucoidan and poly(I), two different
194 scavenger receptor inhibitors, significantly reduced it by 60% and 32%, respectively. Importantly, the
195 inactive analog of poly(I), poly(C), used as a negative control, had no effect on CC17 phagocytosis (Fig.
196 6A). Interestingly, these phenotypes were specific to BM110 since no reduction of NEM316
197 phagocytosis was observed using these two scavenger receptor inhibitors (Fig. 6B). Importantly,
198 fucoidan was also found to reduce BM110 adhesion to THP-1 macrophages whereas it did not reduce
199 NEM316 adhesion (Fig. 6C). These results suggest that some scavenger receptors contribute to a
200 significant proportion of the GBS CC17 adhesion that lead to its uptake into macrophages.

201 Scavenger receptors constitute a large family of membrane-associated pattern recognition receptors
202 (PRRs) that act as receptors mediating direct non-opsonic adhesion and uptake of microbes and/or
203 their products (36). To determine which scavenger receptor(s) contribute(s) to the adhesion/uptake
204 of GBS CC17 in THP-1 macrophages, we characterized by RT-PCR their expression profile in THP-1
205 macrophages. Given that the enhanced phagocytosis of GBS CC17 is conserved in hMDM and
206 monocytes (Fig. 1B, C, D), we extended the analysis of scavenger receptors expression profile to these
207 cell types (Fig. 6D). Using the recent classification of scavenger receptors (37), we identified that, out
208 of the 25 different scavenger receptors tested, 13 were expressed by these three cellular models (Fig.
209 6D). Next, we silenced the expression of each of these 13 individual scavenger receptors by siRNA to
210 address their involvement in GBS CC17 uptake. Efficient knockdown levels were confirmed on two
211 individual genes expressed by THP-1 macrophages for which the knockdown efficiency was 78 and 98
212 % (Fig. S3A). As an additional control, the silencing of the complement receptor impaired the
213 phagocytosis of complemented-red blood cells (96% decreased) (Fig. S3B), demonstrating that siRNA
214 in THP-1 macrophages was efficient. However, when individual scavenger receptors were silenced, no
215 significant reduction in BM110 uptake was observed (Fig. 6E). Last, in agreement with the phagocytosis
216 assays using phagocytosis receptor inhibitors (Fig. 6A), BM110 phagocytosis was not decreased in
217 THP-1 macrophages silenced for FCyR, complement receptors, α5 or β3 integrin expression, Plaur or
218 CD44 (Fig. S3C) or TLRs (Fig. S3D).

219 **CC17 and non-CC17 strains display similar capacity to survive within macrophages**

220 After phagocytosis, the phagocytic vacuole containing bacteria undergoes maturation events leading
221 to the formation of a phagolysosome required for efficient bacterial degradation. GBS is known to
222 survive within macrophages for up to 24 hours (24, 25, 27, 31, 32). In order to gain insight into the
223 physiological relevance of our study, we compared the intracellular fate of BM110 and NEM316 strains
224 in THP-1 macrophages. The maturation of phagosomes containing BM110-GFP and NEM316-GFP
225 (Table S1) was followed by fluorescence microscopy at various time-points after phagocytosis (t=0,
226 t=2h30 and t=5h). BM110 bacteria colocalizing with LAMP-1 and with the Lysotracker (a fluorescent
227 dye labeling acidic organelles such as phagolysosome) were quantified after immunofluorescence
228 staining (Fig. 7A and C). No statistical differences were observed in the kinetic of phagosome
229 maturation between BM110 and NEM316 whatever the time-point (Fig. 7B and D), indicating that the
230 delivery of BM110 and NEM316 to late endosomes or lysosomes is similar.

231 We next compared the survival ability of 10 CC17 and 17 non-CC17 strains clinical isolates by
232 quantifying intracellular viable bacteria 2h30 after phagocytosis (Fig. 7E). Survival results were
233 normalized for each GBS strain to the number of initially phagocytosed bacteria. No significant
234 difference was observed in the survival ability of CC17 and non-CC17 strains (Fig. 7E), whatever the

235 capsular type (Fig. S4A). The survival rate of BM110 and NEM316 strains was also similar 24 h after
236 phagocytosis (Fig. S4B). Consistently, HvgA and Spb1 were not involved in CC17 survival within THP-1
237 macrophages (Fig. 7F) or hMDM (Fig. 7G).

238 Taken together, these results revealed that the intracellular fate of GBS CC17 and non-CC17 after
239 adhesion and phagocytosis is similar.

240 **CC17 and non-CC17 strains can escape macrophages by a passive phenomenon**

241 We next analyzed the capacity of GBS strains to escape THP-1 macrophages. After phagocytosis and
242 antibiotic treatment to eliminate extracellular bacteria, cells were incubated in antibiotic free medium
243 for short periods of time (45 min and 1h30) to allow potential bacterial escape from infected cells
244 without any bacterial multiplication within the extracellular media. GBS egress normalized to the
245 percentage of initial phagocytosis showed that BM110 and NEM316 strains displayed similar capacity
246 to escape from macrophages (Fig. 8A). GBS egress from THP-1 macrophages was neither inhibited by
247 cytochalasin D nor by nocodazole (Fig. 8B), indicating that it is independent of actin cytoskeleton and
248 microtubules, respectively.

249 In conclusion, both strains of GBS can escape from the intracellular compartment to be released into
250 the extracellular compartment at similar rates. Furthermore, bacterial escape is a passive
251 phenomenon, suggesting that escape does not result from the recycling of the bacteria-containing
252 vacuole to the plasma membrane.

253

254 **DISCUSSION**

255 The innate immune response is critical for pathogen clearance, especially in neonates in whom the
256 adaptive immune system is not yet fully mature and the specific antibodies required for adaptive
257 immune response are usually lacking. Phagocytic cells populate all tissues and organs of the body
258 where they play an important role in pathogen clearance.

259 The ability of GBS lineages to interact specifically with phagocytes, particularly their ability to be
260 phagocytosed, remains controversial. In a study using 35 isolates from various GBS lineages, no
261 significant differences were observed in the phagocytosis of GBS strains stratified by capsular serotype
262 or MLST (30). In contrast, a study performed with a more discrete number of GBS isolates (15 GBS
263 strains including 4 CC17 strains) found that CC17 were phagocytosed by macrophages at significantly
264 higher rates than other GBS isolates (32). Our study, performed with a higher number of invasive GBS
265 clinical isolates (27 CC17 isolates and 40 non-CC17 isolates) demonstrates that GBS CC17 strains are
266 more phagocytosed than non-CC17 strains. These conflicting results may be attributed to the use, in
267 the first study, of heat-inactivation of GBS, that could have denatured bacterial surface proteins
268 involved in phagocytosis (30). In agreement with this hypothesis, we demonstrated that the higher
269 phagocytosis of CC17 strains does not depend on the polysaccharidic capsule, a major GBS virulence
270 factor which protects the bacteria from phagocytosis but, rather on the expression of two surface
271 proteins, Spb1, the backbone protein of the PI-2b pilus, and the HvgA adhesin, that promote a higher
272 level of phagocytosis. In contrast, we did not observe any role for the Srr2 surface protein in GBS CC17
273 uptake by macrophages. In agreement with this result, we and others have found that blocking the
274 known Srr2-receptors, α5β1 and αvβ3 integrins, by mimetic peptides (RGD and/or RGfV) or by silencing
275 α5 or β3 integrin expression does not affect CC17 phagocytosis (this study and (23)). Together, these
276 data are consistent and indicate that the Srr2 surface protein is not involved in the uptake of GBS by
277 phagocytes.

278 Importantly, we found that the higher phagocytosis mediated by Spb1 and HvgA was solely the result
279 of an increase of the initial adhesion to phagocytes. Both proteins have previously been described to
280 play a role in adherence to host intestinal epithelial and cerebral endothelial cells (16, 28, 38, 39).
281 Interestingly, in these two cell types, CC17 strains were found to have an approximately 2.5-fold
282 increase in adhesion compared to non-CC17 strains. The increased ability to adhere to both intestinal
283 epithelial and cerebral endothelial cells was found to have physiological functionality, as CC17 strains
284 have a significantly greater ability to colonise the gut and cross the blood-brain barrier (16). Although
285 it is not possible to address *in vivo* whether a 2.3-fold increase in phagocytosis for CC17 strains
286 contributes to the hypervirulence of CC17 strains, our previous data support this hypothesis. After
287 initial adherence to phagocytes, both CC17 and non-CC17 where captured by filopodia and internalized

288 within phagocytes in a process that involved similar signalling molecules. Filopodia formation is known
289 to require the Cdc42 GTPase activity leading to actin polymerization (35). Accordingly, we found that
290 GBS phagocytosis was strongly dependent on actin and Cdc42.

291 While CC17 had a higher adhesion rate, it shared, with non-CC17 strains, a common signaling pathway
292 leading to phagocytosis. This may reflect the recognition of similar cellular receptors - mediating
293 bacterial adhesion and subsequent internalisation of CC17 and non-CC17 strains - but with different
294 affinities. That both strain types interact with the same molecules but with different affinity has
295 previously been described for GBS interaction with fibrinogen which exhibits a 10-fold higher affinity
296 for CC17 strains than for non-CC17 strains (40). Alternatively, it may reflect an internalisation process
297 in a two-step mechanism involving a *sensus stricto* adhesion receptor followed by engulfment
298 mediated by a phagocytic receptor. In this scenario, CC17 or non-CC17 strains would recognise
299 different adhesion receptors, while the internalisation process would involve a common phagocytic
300 receptor. Two-step phagocytosis mechanisms have previously been described involving cross-talk
301 between TLRs and scavenger receptors (41, 42).

302 The identity of the cellular receptor(s) involved in the non-opsonized phagocytosis of GBS has been
303 carried out by many teams (22, 23, 43). Despite these efforts, such receptor(s) are still unknown. Our
304 study indicates that FcyRs, complement receptors and CD14 are not involved in the phagocytosis of
305 non-opsonized GBS, as described previously (22, 23, 43). Accordingly, GBS phagocytosis is independent
306 of Syk and Rock kinases that are known to be involved in FCyR and complement receptor signalling,
307 respectively (44). Interestingly, fucoidan and poly(I), two broad scavenger receptor inhibitors reduced
308 the phagocytosis of the BM110 CC17 strain, while having no significant effect on the adhesion and
309 phagocytosis of a non-CC17 strain. Scavenger receptors are a diverse family of proteins that recognize
310 polyanionic ligands and can act as PRR involved in the recognition of various microbial ligands as well
311 as in their phagocytosis (45). The polynucleotide ligand poly(I) acts by efficient competitive inhibition
312 of the binding of other polyanionic ligands to the cationic collagenous binding domain of some
313 scavenger receptors. Similarly, fucoidan easily interacts with positively charged molecules because of
314 its high negative charge at neutral pH (46, 47). These molecules have been successfully used to inhibit
315 adhesion and/or phagocytosis of several pathogens (48, 49). The inhibitory effect of fucoidan and
316 poly(I) on CC17 adhesion and phagocytosis led us to conclude that scavenger receptor(s) might be
317 involved in the adhesion and/or uptake of non-opsonized CC17 bacteria by macrophages. Since
318 scavenger receptors have a wide distribution, being expressed by phagocytes as well as by epithelial
319 and endothelial cells (37), it is tempting to speculate that Spb1 and HvgA promote adhesion to host
320 cells by recognizing the same receptors on phagocytes, epithelial and endothelial cells. Interestingly, it
321 has been recently described that the scavenger receptor SSC4D, expressed by phagocytes and

322 epithelial cells, interacts with BM110 strain (50). SSCD4 is a secreted scavenger receptor making this
323 molecule unlikely to be involved in the initial adherence of CC17 bacteria to the macrophage surface.
324 In addition, silencing SSC4D expression does not affect CC17 phagocytosis (not shown) confirming its
325 absence of involvement in this phenotype. Despite our efforts, the siRNA screen performed to identify
326 scavenger receptor(s) involved in GBS uptake was unsuccessful. Several hypotheses could explain this
327 failure. Because CC17 increased phagocytosis is a phenotype conserved between macrophages and
328 monocytes from cell lines and primary cells, we hypothesized that the receptor(s) involved in CC17
329 adhesion/phagocytosis is also conserved in these different cell types. However, we cannot exclude the
330 possibility that different scavenger receptors in each cellular model allow CC17 uptake, or that several
331 scavenger receptors have a cooperative effect. Also, the list of scavenger receptors is constantly
332 growing and we might have missed the scavenger receptor(s) involved in GBS CC17
333 adhesion/phagocytosis. Finally, we cannot exclude a non-specific or an indirect effect of fucoidan and
334 poly(I) on the signaling of others PRRs, as described previously (51).

335 Numerous pathogens have evolved sophisticated strategies to avoid capture and/or killing by
336 phagocytes. GBS efficiently survive within phagocytes by expressing multiple bacterial factors involved
337 in acid stress response and ROS resistance, including the orange carotenoid pigment hemolysin, the
338 glutathione or the superoxide dismutase (SodA) (26, 52). The capacity of different GBS lineages to
339 survive within macrophages has been controversial (25, 27, 31, 32). The discrepancies between the
340 different studies likely come from either the low number of bacterial strains tested or to the calculation
341 of survival rate (25, 27, 31, 32). Indeed, depending on whether the intracellular survival ability is related
342 to the number of phagocytosed bacteria (intracellular bacteria at T0) or to the initial bacterial inoculum
343 different results will be obtained. As CC17 strains display higher adhesion level leading to higher initial
344 load of intracellular CC17 this might *in fine* lead to a higher recovering number of intracellular bacteria
345 at later time points. By calculating the survival rate in relation to the number of phagocytosed bacteria,
346 we found that CC17 and non-CC17 strains display similar intracellular fate with similar survival capacity.
347 In agreement with this result, we found that Sbp1 and HvgA proteins do not contribute to intracellular
348 survival. We also showed that after internalisation, bacteria can be released into the external
349 compartment. As observed for bacterial survival, we found that bacterial egress of CC17 and non-CC17
350 strains occurs at a similar rate when normalised to the initially phagocytised bacteria. However, due
351 to enhanced phagocytosis of CC17 strains, this results in a greater number of bacteria being released
352 into the extracellular compartment. Interestingly, we found that bacterial egress occurs even when
353 actin or microtubule networks are disrupted. Since most vacuolar movements involve the
354 cytoskeleton, this suggests that GBS release into the extracellular compartment is a passive

355 phenomenon that may be due to spontaneous macrophage lysis. Further studies are needed to
356 confirm this hypothesis.
357 The hypervirulent CC17 clone is strongly associated with LOD (60% to 80% of the cases) for which the
358 gastrointestinal tract is likely to be the portal of entry. In the gut, CC17 strains can transcytose *via* M
359 cells and are found associated with CD11c - a marker for macrophages and dendritic cells - positive
360 cells in the Peyer's patches (8). Interestingly, an increased proportion of CD11c positive cells have been
361 found in the mesenteric lymph node of CC17-infected mice (8). This suggests that CD11c positive cells
362 may act as Trojan horses, to promote the dissemination of CC17 bacteria in the gut. In addition, the
363 higher CC17 intracellular load could also contribute to the establishment of a survival niche and
364 bacterial persistence in tissues.

365 In conclusion, the specific features associated with the interaction between the CC17 lineage and the
366 phagocytes likely contribute to its particular virulence and to the pathophysiology of infection. Indeed,
367 the increased CC17 bacterial loads in macrophages may confer a selective advantage to promote better
368 persistence and dissemination.

369 **MATERIALS AND METHODS**

370 **Bacterial strains**

371 Bacterial strains used in this study are listed in Table S1. GBS BM110 (CC17) and NEM316 (CC23) are
372 well characterized capsular serotype III strains isolated from blood cultures of neonates (16). BM110
373 and NEM316 were used as CC17 and non-CC17 reference strains, respectively. Other GBS clinical
374 strains isolated from invasive infections (*i.e*. from blood culture, cerebrospinal fluid or other normally
375 sterile sites) were obtained from the French National Reference Center for Streptococci
376 (http://www.cnr-strep.fr). Capsular genotyping and MLST was performed for all GBS strains (Table S2).
377 All bacterial strains were cultured in Todd Hewitt (TH) broth or agar (Difco Laboratories, Detroit, MI)
378 at 37°C, except for *L. lactis* which was grown at 30°C. When necessary, antibiotics were used to
379 maintain plasmids at the following concentrations, spectinomycin 100 $\mu g.mL^{-1}$, erythromycin 10
380 $\mu g.mL^{-1}$.

381 **THP-1 cell line and culture conditions**

382 THP-1 (TIB-202 from ATCC) cell line is a spontaneous immortalized monocyte-like cell line, derived
383 from the peripheral blood of a childhood case of acute monocytic leukemia. THP-1 cells were cultured
384 at 37°C under a 5% CO_2 atmosphere in RPMI1640 + Glutamax (Gibco), 10% Fetal Calf Serum (FCS, Gibco)
385 and 0.05 mM β-mercapto-ethanol. Cells were passaged twice per week and kept at a cell concentration
386 below 1×10^6 cells /mL. THP-1 cell line was routinely tested for mycoplasma contamination (Mycoalert
387 mycoplasma detection kit, LONZA). To differentiate monocytic THP-1 into adherent macrophages, cells
388 were seeded in 24-well plates at 3×10^5 cells per well in culture media containing 200 nM phorbol 12-
389 myristate 13-acetate (PMA) during 3 days, then media was replaced by fresh RPMI1640 complete
390 media without PMA. Cells were incubated for an additional 5 days without any medium change to
391 allow complete differentiation into macrophages as described previously (53).

392 **Isolation and culture of primary human Peripheral Blood Mononuclear Cells (PBMCs) and**
393 **Monocytes-Derived Macrophages (hMDMs)**

394 Blood of adult healthy donors was used (Etablissement Français du Sang, Ile de France, Site Saint-
395 Antoine-le Crozatier) with the appropriate ethics prior approval as stated in the EFS/ INSERM
396 agreement #18EFS030, ensuring that all donors gave a written informed consent and providing
397 anonymized samples. Primary human monocytes were negatively selected using the EasySep Human
398 Monocyte enrichment kit (StemCell®) following the manufacturer's instructions. For hMDM, primary
399 human PBMCs were isolated by density gradient sedimentation in Histopaque® (Sigma) according to
400 the manufacturer's recommendations. Monocytes were then selected by adhesion to dishes for 2 h at
401 37°C in FCS-free medium (RPMI 1640 medium supplemented with 0.1 $mg.ml^{-1}$ gentamicin). Monocytes

402 were differentiated into hMDMs for at least 7 days in complete medium containing 10 $ng.mL^{-1}$ of
403 recombinant human macrophage colony-stimulating factor (rhM-CSF; R&D systems).

404 **Phagocytosis and survival assay in monocytes and macrophages**

405 Monocytes and macrophages from THP-1 cell line and primary cells were used to study the
406 phagocytosis and the intracellular survival of GBS strains. All experiments were carried out with GBS
407 strains grown to mid-log phase and washed twice with sterile Phosphate buffer saline (PBS) before
408 infection. After addition of bacteria, a quick centrifugation (5 min, 200 × g) was performed to
409 synchronize infection. Phagocytes were infected for 45 min at 37°C and under a 5% CO_2 atmosphere
410 in RPMI 1640 medium with GBS strains, using a multiplicity of infection (MOI) of 10 bacteria per cell
411 except when otherwise specified. After infection, phagocytes were washed 3 times with PBS.
412 Remaining extracellular bacteria were killed using RPMI 1640 medium supplemented with Penicillin G
413 / Streptomycin (100 $units.mL^{-1}$ / 0.1 $mg.mL^{-1}$) and Gentamicin (0.2 $mg.mL^{-1}$) at 37°C and 5% CO_2. After
414 antibiotic treatment, cells were washed twice and either lysed directly by osmotic choc using sterile
415 ice-cold H_2O to evaluate phagocytosis (T0) or further incubated in RPMI1640 medium to follow
416 intracellular survival before being lysed (2h30 or 24h). Serial dilutions of the lysates were plated onto
417 TH agar for colony forming units (CFU) counting. The percentage of phagocytosis was calculated as
418 follows: (CFU phagocytosis / CFU in inoculum) × 100. The percentage of survival was calculated as
419 follows: (CFU survival / CFU phagocytosis) × 100. When specified, results were expressed as normalized
420 to the control strain (BM110). Assays were performed in triplicate and were repeated at least three
421 times.

422 **Adhesion assay onto monocytes and macrophages**

423 For adhesion assays, infection was performed as described for phagocytosis but at 4°C and with ice-
424 cold RPMI1640 medium to avoid engulfment of bacteria and phagocytosis. In some experiments,
425 adhesion was also tested at 37°C using cells that had been pre-treated for 1 hour with cytochalasin D.
426 After 3 washes with ice-cold PBS to remove non-adherent bacteria, phagocytes were directly lysed by
427 osmotic shock with ice-cold H_2O. Serial dilutions of lysates were then plated onto TH agar for CFU
428 counting. The percentage of adhesion was determined by calculating the ratio between the CFUs of
429 adherent bacteria and the CFUs from the inoculum × 100. When specified, results were expressed as
430 normalized to the control strain. Assays were performed in triplicate and were repeated at least three
431 times.

432 **Phagocytosis assay in the presence of inhibitors/reagents**

433 Selected compounds were tested for their ability to block GBS phagocytosis. All inhibitors and reagents
434 used in this study are listed in Table S3. THP-1 macrophages were pretreated with inhibitors/reagents

435 for 1h prior infection with BM110 or NEM316 strains. Inhibitors/reagents were left during the time of
436 infection at the same concentration. Treatments did not affect bacterial or cell viability as assessed by
437 Lactate dehydrogenase release in the culture supernatant (LDH cytotoxicity kit®, Promega, according
438 to the manufacturer's instructions; data not shown). The percentage of phagocytosis was calculated
439 as follows: (CFU phagocytosis / CFU in inoculum) × 100 and results were normalized to the untreated
440 condition.

441 **Evaluation of bacterial egress from macrophages**

442 To assess bacterial egress from macrophages, cells were infected as described previously, and then
443 treated with antibiotics to kill extracellular bacteria for 45 min. Cells culture medium was next replaced
444 by medium without any antibiotic. Bacterial egress was quantified in the supernatant of infected
445 macrophages after 45 min or after 1h30 following the replacement of the cell culture medium. The
446 percent of bacterial egress was calculated as follows: (CFU released bacteria / CFU phagocytosed) ×
447 100.

448 **RNA extraction, cDNA synthesis and RT-PCR**

449 RNAs were extracted from non-infected THP-1 macrophages, monocytes and hMDM using the
450 NucleoSpin® RNA kit (Macherey-Nagel®) according to the manufacturer's instructions. RNA
451 concentration was determined using a NanoDrop 2000 spectrophotometer. Then, 1 µg RNA was
452 reverse-transcribed into cDNA using the SuperScript® IV Reverse Transcription Kit (Invitrogen),
453 following the manufacturer's instructions. PCR were carried out with Green Taq DNA polymerase
454 (Promega) on cDNA using primers described in Table S4. Primers were designed in order to amplify all
455 variants of the targeted receptor(s). Amplification products were resolved in 1% (w/v) agarose gel.

456 **siRNA transfection**

457 To silence the expression of putative phagocytic receptors, pools of three or four siRNA duplexes
458 (Dharmacon) were used. The silencer select-negative control-1 siRNA (Ambion) was used as negative
459 control. THP-1 were seeded in twenty-four-well plates for 24 h in the presence of 200 nM of PMA then
460 transfected with 50 nM siRNA using Lipofectamine RNAIMAX (Invitrogen) according to the
461 manufacturer's instructions and incubated for a further 3 days. Efficiency of knockdown was assessed
462 by Western Blot analysis on 2 independent targets.

463 **Immunofluorescent staining and image analysis**

464 To follow intracellular fate of GBS strains, THP-1 macrophages were infected for 45 minutes as
465 described for phagocytosis then washed extensively and fixed at different time points post-
466 phagocytosis (0, 2h30 or 5h) on glass coverslips with 4% paraformaldehyde (PFA) for 10 min then

467 washed with PBS. Following fixation, samples were permeabilized and saturated with PBS containing
468 0.2% saponin and 10% serum for 1h at room temperature, then incubated for at least 1h at room
469 temperature with the primary anti-LAMP1 antibody (DSHB clone H4A3). After 3 washes with PBS,
470 samples were incubated for 1h at room temperature with conjugated-secondary antibodies (Jackson
471 ImmunoResearch Laboratories).

472 To enable detection of acidic compartments (phagolysosome), THP-1 macrophages were incubated 30
473 min before the end of infection with Lysotracker red DND-99 (Invitrogen) at a final concentration of 75
474 nM, fixed with 4% PFA for 10 min, then washed with PBS.

475 After 3 washes in PBS, coverslips were mounted in DAKO fluorescent mounting media (DAKO). Image
476 acquisitions were realized using confocal laser scanning microscopy (Leica DMI6000) coupled to a
477 spinning disk confocal head (YokogawaCSU-X1M1), controlled by the Metamorph 7.7.5 software
478 (Cochin Institute microscopy facility, IMAG'IC). Images were processed using the ImageJ software. At
479 least 300 cells were analyzed for each sample in four independent experiments.

480 **Scanning Electron Microscopy**

481 All incubations were performed at room temperature except when otherwise indicated. Macrophages
482 grown on glass coverslips were infected as described previously and then fixed in 0.1M sodium
483 cacodylate buffer, pH 7.4 containing 2.5% glutaraldehyde and 1% PFA for 60 min. After washing in
484 cacodylate buffer (2x10 min), cells were fixed in 1% OsO_4 diluted in cacodylate buffer for 45 min at 4°C.
485 After washing in cacodylate buffer (2x10 min), samples were dehydrated in an ascending series of
486 ethanol (30%, 50%, 70%, 95%, 100%, 100%, 100% - 10 min each), followed by hexamethyldisilazane
487 /ethanol (1/1) for 10 min and hexamethyldisilazane for 10 min. After overnight air drying, each
488 coverslip was placed on a double-sided sticky tape on the top of an aluminum stub and sputter coated
489 with Au/Pd. Images were acquired using a Jeol LV6510 (Jeol, Croissy-sur-Seine, France).

490 **Statistical analysis**

491 All assays were performed in at least in three independent experiments, each experiment was carried
492 out in triplicate. Data represent mean ± SEM or median and statistical analyses were performed using
493 GraphPad Prism 10.0 (GraphPad Software, San Diego, California). Significance levels were set at $*p \leq$
494 0.05; $**p \leq 0.01$; $***p \leq 0.001$; $****\ p \leq 0.0001$.

495

496 **AUTHOR CONTRIBUTIONS**

497 JG designed the research. ASB, AP, JCF, CH and JG performed the experiments. ASB, AP, JG analyzed
498 the data. BS and VM performed electron microscopy experiments. AF, AT, CP provided intellectual
499 input and guidance. JG wrote the manuscript and ASB, AF, AT contributed to finalizing the manuscript.
500 All authors discussed results and reviewed the final version of the manuscript.

501 **ACKNOWLEDGMENTS**

502 We are grateful to Glen Ulett for the gift of the GFP plasmid. We thank Cristina Candeias for technical
503 assistance, Shaynoor Dramsi for BM110Δ*spb1* and NEM316Δ*cps* mutant strains and the Imag'IC core
504 facility of the Cochin Institute. The H4A3 antibody developed by August, J.T. / Hildreth, J.E.K. was
505 obtained from the Developmental Studies Hybridoma Bank, created by the NICHD of the NIH and
506 maintained at The University of Iowa, Department of Biology, Iowa City, IA 52242.

507 **FINANCIAL SUPPORT**

508 This work was supported by Agence Nationale de la Recherche (ANR) (Grant StrepB2brain, ANR-17-
509 CE15-0026-01). ASB was a doctoral fellow funded by Université Paris Cité.

510

511 **REFERENCES**

512 1. Marodi L. 2006. Neonatal innate immunity to infectious agents. Infect Immun 74:1999-2006.
513 2. Mittal R, Sukumaran SK, Selvaraj SK, Wooster DG, Babu MM, Schreiber AD, Verbeek JS,
514 Prasadarao NV. 2010. Fcgamma receptor I alpha chain (CD64) expression in macrophages is
515 critical for the onset of meningitis by Escherichia coli K1. PLoS Pathog 6:e1001203.
516 3. Orrskog S, Rounioja S, Spadafina T, Gallotta M, Norman M, Hentrich K, Falker S, Ygberg-
517 Eriksson S, Hasenberg M, Johansson B, Uotila LM, Gahmberg CG, Barocchi M, Gunzer M,
518 Normark S, Henriques-Normark B. 2013. Pilus adhesin RrgA interacts with complement
519 receptor 3, thereby affecting macrophage function and systemic pneumococcal disease. MBio
520 4:e00535-12.
521 4. Rosales C, Uribe-Querol E. 2017. Phagocytosis: A Fundamental Process in Immunity. Biomed
522 Res Int 2017:9042851.
523 5. Patras KA, Nizet V. 2018. Group B Streptococcal Maternal Colonization and Neonatal Disease:
524 Molecular Mechanisms and Preventative Approaches. Front Pediatr 6:27.
525 6. Seale AC, Bianchi-Jassir F, Russell NJ, Kohli-Lynch M, Tann CJ, Hall J, Madrid L, Blencowe H,
526 Cousens S, Baker CJ, Bartlett L, Cutland C, Gravett MG, Heath PT, Ip M, Le Doare K, Madhi SA,
527 Rubens CE, Saha SK, Schrag SJ, Sobanjo-Ter Meulen A, Vekemans J, Lawn JE. 2017. Estimates
528 of the Burden of Group B Streptococcal Disease Worldwide for Pregnant Women, Stillbirths,
529 and Children. Clin Infect Dis 65:S200-S219.
530 7. Tazi A, Plainvert C, Anselem O, Ballon M, Marcou V, Seco A, El Alaoui F, Joubrel C, El Helali N,
531 Falloukh E, Frigo A, Raymond J, Trieu-Cuot P, Branger C, Le Monnier A, Azria E, Ancel PY, Jarreau
532 PH, Mandelbrot L, Goffinet F, Poyart C. 2019. Risk Factors for Infant Colonization by
533 Hypervirulent CC17 Group B *Streptococcus*: Toward the Understanding of Late-onset Disease.
534 Clin Infect Dis doi:ciz033 [pii] 10.1093/cid/ciz033 5427769 [pii].
535 8. Hays C, Touak G, Bouaboud A, Fouet A, Guignot J, Poyart C, Tazi A. 2019. Perinatal hormones
536 favor CC17 group B *Streptococcus* intestinal translocation through M cells and hypervirulence
537 in neonates. Elife 8.
538 9. Madrid L, Seale AC, Kohli-Lynch M, Edmond KM, Lawn JE, Heath PT, Madhi SA, Baker CJ,
539 Bartlett L, Cutland C, Gravett MG, Ip M, Le Doare K, Rubens CE, Saha SK, Sobanjo-Ter Meulen
540 A, Vekemans J, Schrag S, Infant GBSDIG. 2017. Infant Group B Streptococcal Disease Incidence
541 and Serotypes Worldwide: Systematic Review and Meta-analyses. Clin Infect Dis 65:S160-S172.
542 10. Joubrel C, Tazi A, Six A, Dmytruk N, Touak G, Bidet P, Raymond J, Trieu Cuot P, Fouet A, Kerneis
543 S, Poyart C. 2015. Group B *Streptococcus* neonatal invasive infections, France 2007-2012. Clin
544 Microbiol Infect 21:910-6.
545 11. Vuillemin X, Hays C, Plainvert C, Dmytruk N, Louis M, Touak G, Saint-Pierre B, Adoux L,
546 Letourneur F, Frigo A, Poyart C, Tazi A. 2021. Invasive group B *Streptococcus* infections in non-
547 pregnant adults: a retrospective study, France, 2007-2019. Clin Microbiol Infect 27:129 e1-129
548 e4.
549 12. Manning SD, Springman AC, Lehotzky E, Lewis MA, Whittam TS, Davies HD. 2009. Multilocus
550 sequence types associated with neonatal group B streptococcal sepsis and meningitis in
551 Canada. J Clin Microbiol 47:1143-8.
552 13. Teatero S, McGeer A, Low DE, Li A, Demczuk W, Martin I, Fittipaldi N. 2014. Characterization
553 of invasive group B *Streptococcus* strains from the greater Toronto area, Canada. J Clin
554 Microbiol 52:1441-7.
555 14. van Kassel M, de Boer G, Teeri S, Jamrozy D, Bentley S, Brouwer M, Van der Ende A, Van de
556 Beek D, Bijlsma M. 2021. Molecular epidemiology and mortality of group B streptococcal
557 meningitis and infant sepsis in the Netherlands: a 30-year nationwide surveillance study. The
558 lancet microbe 2.
559 15. Brochet M, Couve E, Zouine M, Vallaeys T, Rusniok C, Lamy MC, Buchrieser C, Trieu-Cuot P,
560 Kunst F, Poyart C, Glaser P. 2006. Genomic diversity and evolution within the species
561 *Streptococcus agalactiae*. Microbes Infect 8:1227-43.

562 16. Tazi A, Disson O, Bellais S, Bouaboud A, Dmytruk N, Dramsi S, Mistou MY, Khun H, Mechler C,
563 Tardieux I, Trieu-Cuot P, Lecuit M, Poyart C. 2010. The surface protein HvgA mediates group B
564 *Streptococcus* hypervirulence and meningeal tropism in neonates. J Exp Med 207:2313-22.
565 17. Deshayes de Cambronne R, Fouet A, Picart A, Bourrel AS, Anjou C, Bouvier G, Candeias C,
566 Bouaboud A, Costa L, Boulay AC, Cohen-Salmon M, Plu I, Rambaud C, Faurobert E, Albiges-Rizo
567 C, Tazi A, Poyart C, Guignot J. 2021. CC17 group B *Streptococcus* exploits integrins for neonatal
568 meningitis development. J Clin Invest 131.
569 18. Springman AC, Lacher DW, Wu G, Milton N, Whittam TS, Davies HD, Manning SD. 2009.
570 Selection, recombination, and virulence gene diversity among group B streptococcal
571 genotypes. J Bacteriol 191:5419-27.
572 19. Korir ML, Manning SD, Davies HD. 2017. Intrinsic Maturational Neonatal Immune Deficiencies
573 and Susceptibility to Group B *Streptococcus* Infection. Clin Microbiol Rev 30:973-989.
574 20. Chang YC, Nizet V. 2020. Siglecs at the Host-Pathogen Interface. Adv Exp Med Biol 1204:197-
575 214.
576 21. Marques MB, Kasper DL, Pangburn MK, Wessels MR. 1992. Prevention of C3 deposition by
577 capsular polysaccharide is a virulence mechanism of type III group B streptococci. Infect
578 Immun 60:3986-93.
579 22. Henneke P, Takeuchi O, Malley R, Lien E, Ingalls RR, Freeman MW, Mayadas T, Nizet V, Akira
580 S, Kasper DL, Golenbock DT. 2002. Cellular activation, phagocytosis, and bactericidal activity
581 against group B *Streptococcus* involve parallel myeloid differentiation factor 88-dependent
582 and independent signaling pathways. J Immunol 169:3970-7.
583 23. Valentin-Weigand P, Benkel P, Rohde M, Chhatwal GS. 1996. Entry and intracellular survival of
584 group B streptococci in J774 macrophages. Infect Immun 64:2467-73.
585 24. Cornacchione P, Scaringi L, Fettucciari K, Rosati E, Sabatini R, Orefici G, von Hunolstein C,
586 Modesti A, Modica A, Minelli F, Marconi P. 1998. Group B streptococci persist inside
587 macrophages. Immunology 93:86-95.
588 25. Cumley NJ, Smith LM, Anthony M, May RC. 2012. The CovS/CovR acid response regulator is
589 required for intracellular survival of group B *Streptococcus* in macrophages. Infect Immun
590 80:1650-61.
591 26. Sullivan MJ, Prince D, Goh KGK, Katupitiya L, Gosling D, Crowley MR, Crossman DK, Ulett GC.
592 2023. Dual RNA sequencing of group B *Streptococcus*-infected human monocytes reveals new
593 insights into host-pathogen interactions and bacterial evasion of phagocytosis. Sci Rep
594 13:2137.
595 27. Chattopadhyay D, Carey AJ, Caliot E, Webb RI, Layton JR, Wang Y, Bohnsack JF, Adderson EE,
596 Ulett GC. 2011. Phylogenetic lineage and pilus protein Spb1/SAN1518 affect opsonin-
597 independent phagocytosis and intracellular survival of Group B *Streptococcus*. Microbes Infect
598 13:369-82.
599 28. Perichon B, Guignot J, Szili N, Gao C, Poyart C, Trieu-Cuot P, Dramsi S. 2019. Insights into
600 *Streptococcus agalactiae* PI-2b pilus biosynthesis and role in adherence to host cells. Microbes
601 Infect 21:99-103.
602 29. Six A, Bellais S, Bouaboud A, Fouet A, Gabriel C, Tazi A, Dramsi S, Trieu-Cuot P, Poyart C. 2015.
603 Srr2, a multifaceted adhesin expressed by ST-17 hypervirulent Group B *Streptococcus* involved
604 in binding to both fibrinogen and plasminogen. Mol Microbiol 97:1209-22.
605 30. Rogers LM, Gaddy JA, Manning SD, Aronoff DM. 2018. Variation in Macrophage Phagocytosis
606 of *Streptococcus agalactiae* Does Not Reflect Bacterial Capsular Serotype, Multilocus
607 Sequence Type, or Association with Invasive Infection. Pathog Immun 3:63-71.
608 31. Korir ML, Laut C, Rogers LM, Plemmons JA, Aronoff DM, Manning SD. 2017. Differing
609 mechanisms of surviving phagosomal stress among group B *Streptococcus* strains of varying
610 genotypes. Virulence 8:924-937.
611 32. Flaherty RA, Aronoff DM, Gaddy JA, Petroff MG, Manning SD. 2021. Distinct Group B
612 *Streptococcus* Sequence and Capsule Types Differentially Impact Macrophage Stress and
613 Inflammatory Signaling Responses. Infect Immun 89.

614 33. Perichon B, Szili N, du Merle L, Rosinski-Chupin I, Gominet M, Bellais S, Poyart C, Trieu-Cuot P,
615 Dramsi S. 2017. Regulation of PI-2b Pilus Expression in Hypervirulent *Streptococcus agalactiae*
616 ST-17 BM110. PLoS One 12:e0169840.
617 34. Uribe-Querol E, Rosales C. 2020. Phagocytosis: Our Current Understanding of a Universal
618 Biological Process. Front Immunol 11:1066.
619 35. Krugmann S, Jordens I, Gevaert K, Driessens M, Vandekerckhove J, Hall A. 2001. Cdc42 induces
620 filopodia by promoting the formation of an IRSp53:Mena complex. Curr Biol 11:1645-55.
621 36. Pombinho R, Sousa S, Cabanes D. 2018. Scavenger Receptors: Promiscuous Players during
622 Microbial Pathogenesis. Crit Rev Microbiol 44:685-700.
623 37. PrabhuDas MR, Baldwin CL, Bollyky PL, Bowdish DME, Drickamer K, Febbraio M, Herz J, Kobzik
624 L, Krieger M, Loike J, McVicker B, Means TK, Moestrup SK, Post SR, Sawamura T, Silverstein S,
625 Speth RC, Telfer JC, Thiele GM, Wang XY, Wright SD, El Khoury J. 2017. A Consensus Definitive
626 Classification of Scavenger Receptors and Their Roles in Health and Disease. J Immunol
627 198:3775-3789.
628 38. Adderson EE, Takahashi S, Wang Y, Armstrong J, Miller DV, Bohnsack JF. 2003. Subtractive
629 hybridization identifies a novel predicted protein mediating epithelial cell invasion by virulent
630 serotype III group B *Streptococcus agalactiae*. Infect Immun 71:6857-63.
631 39. Sharma P, Lata H, Arya DK, Kashyap AK, Kumar H, Dua M, Ali A, Johri AK. 2013. Role of pilus
632 proteins in adherence and invasion of *Streptococcus agalactiae* to the lung and cervical
633 epithelial cells. J Biol Chem 288:4023-34.
634 40. Seo HS, Minasov G, Seepersaud R, Doran KS, Dubrovska I, Shuvalova L, Anderson WF, Iverson
635 TM, Sullam PM. 2013. Characterization of fibrinogen binding by glycoproteins Srr1 and Srr2 of
636 *Streptococcus agalactiae*. J Biol Chem 288:35982-96.
637 41. Doyle SE, O'Connell RM, Miranda GA, Vaidya SA, Chow EK, Liu PT, Suzuki S, Suzuki N, Modlin
638 RL, Yeh WC, Lane TF, Cheng G. 2004. Toll-like receptors induce a phagocytic gene program
639 through p38. J Exp Med 199:81-90.
640 42. Amiel E, Alonso A, Uematsu S, Akira S, Poynter ME, Berwin B. 2009. Pivotal Advance: Toll-like
641 receptor regulation of scavenger receptor-A-mediated phagocytosis. J Leukoc Biol 85:595-605.
642 43. Albanyan EA, Vallejo JG, Smith CW, Edwards MS. 2000. Nonopsonic binding of type III Group B
643 Streptococci to human neutrophils induces interleukin-8 release mediated by the p38
644 mitogen-activated protein kinase pathway. Infect Immun 68:2053-60.
645 44. Lee HJ, Woo Y, Hahn TW, Jung YM, Jung YJ. 2020. Formation and Maturation of the
646 Phagosome: A Key Mechanism in Innate Immunity against Intracellular Bacterial Infection.
647 Microorganisms 8.
648 45. Taban Q, Mumtaz PT, Masoodi KZ, Haq E, Ahmad SM. 2022. Scavenger receptors in host
649 defense: from functional aspects to mode of action. Cell Commun Signal 20:2.
650 46. Lin Z, Tan X, Zhang Y, Li F, Luo P, Liu H. 2020. Molecular Targets and Related Biologic Activities
651 of Fucoidan: A Review. Mar Drugs 18.
652 47. Sigola LB, Fuentes AL, Millis LM, Vapenik J, Murira A. 2016. Effects of Toll-like receptor ligands
653 on RAW 264.7 macrophage morphology and zymosan phagocytosis. Tissue Cell 48:389-96.
654 48. Baba M, Snoeck R, Pauwels R, de Clercq E. 1988. Sulfated polysaccharides are potent and
655 selective inhibitors of various enveloped viruses, including herpes simplex virus,
656 cytomegalovirus, vesicular stomatitis virus, and human immunodeficiency virus. Antimicrob
657 Agents Chemother 32:1742-5.
658 49. Thelen T, Hao Y, Medeiros AI, Curtis JL, Serezani CH, Kobzik L, Harris LH, Aronoff DM. 2010. The
659 class A scavenger receptor, macrophage receptor with collagenous structure, is the major
660 phagocytic receptor for *Clostridium sordellii* expressed by human decidual macrophages. J
661 Immunol 185:4328-35.
662 50. Cardoso MS, Santos RF, Almeida S, Sa M, Perez-Cabezas B, Oliveira L, Tavares J, Carmo AM.
663 2021. Physical Interactions With Bacteria and Protozoan Parasites Establish the Scavenger
664 Receptor SSC4D as a Broad-Spectrum Pattern Recognition Receptor. Front Immunol
665 12:760770.

666 51. Dutot M, Grassin-Delyle S, Salvator H, Brollo M, Rat P, Fagon R, Naline E, Devillier P. 2019. A
667 marine-sourced fucoidan solution inhibits Toll-like-receptor-3-induced cytokine release by
668 human bronchial epithelial cells. Int J Biol Macromol 130:429-436.
669 52. Shabayek S, Spellerberg B. 2017. Acid Stress Response Mechanisms of Group B Streptococci.
670 Front Cell Infect Microbiol 7:395.
671 53. Daigneault M, Preston JA, Marriott HM, Whyte MK, Dockrell DH. 2010. The identification of
672 markers of macrophage differentiation in PMA-stimulated THP-1 cells and monocyte-derived
673 macrophages. PLoS One 5:e8668.

674

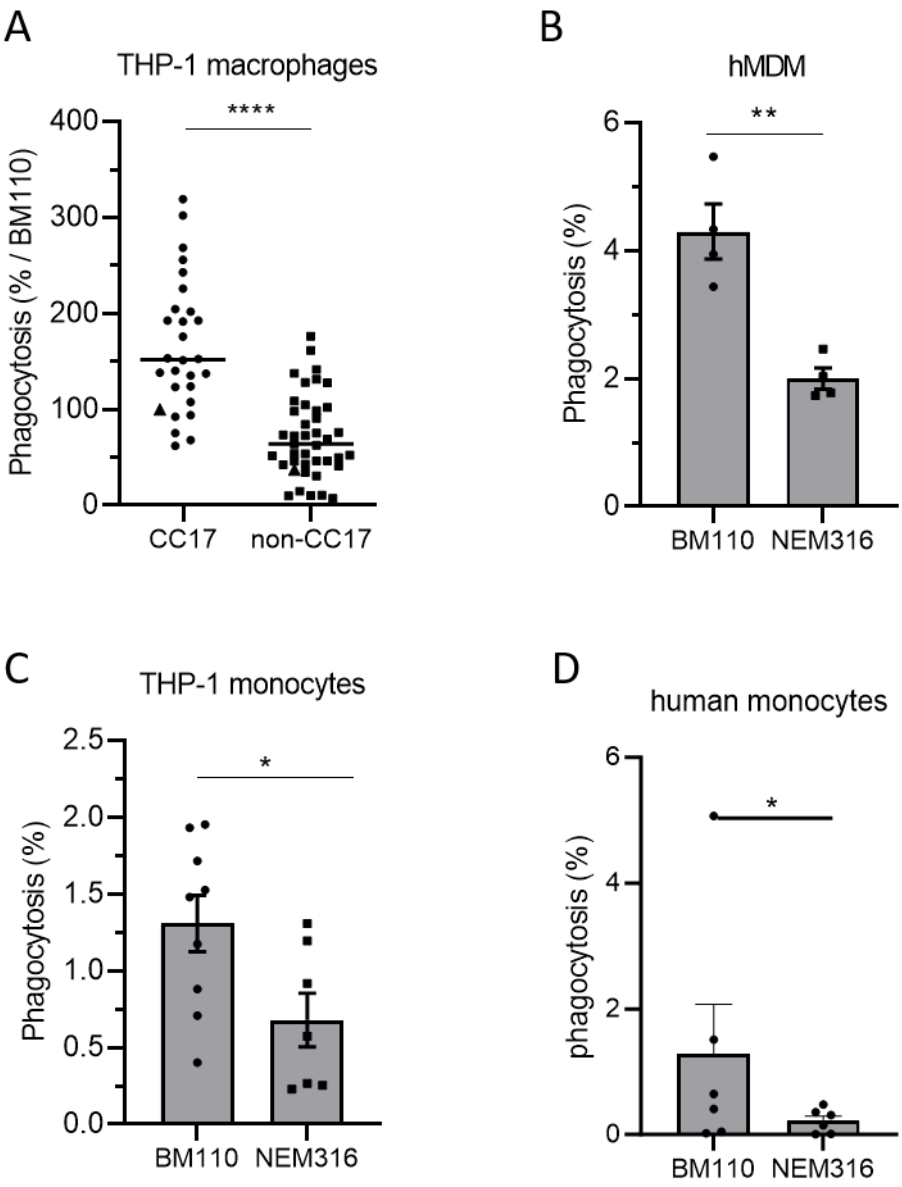

675

676 **Figure 1: CC17 GBS strains are more phagocytosed by monocytes and macrophages than non-CC17**
677 **GBS strains.** (A, B, C, D) Phagocytosis level of GBS strains was assessed by CFU count after infection at
678 MOI 10 followed by antibiotic treatment to kill extracellular bacteria using (A) THP-1 macrophages (B)
679 hMDM primary cells, (C) THP-1 monocytes or (D) human primary monocytes. (A) Phagocytes were
680 infected with CC17 and non-CC17 GBS clinical isolates from invasive infections, each dot representing
681 a clinical strain. Triangles correspond to BM110 strain (CC17) and NEM316 (non-CC17). Results are
682 expressed as the percentage of phagocytosis relative to BM110 strain phagocytosis, with horizontal
683 lines indicating median value. (B, C, D) Phagocytes were infected with GBS strains BM110 and NEM316.
684 Results are expressed as the percentage of phagocytosed bacteria normalized to (B, C) the initial
685 inoculum or (D) to BM110 strain phagocytosis.

686 Statistical analysis: data shown are (A) median or (B, C, D) mean ± SEM of at least four independent
687 experiments. (A, B, C) t test or (D) Mann Whitney test, were performed with *, $p < 0.05$; **, $p < 0.01$;
688 ****, $p < 0.0001$.

689

690

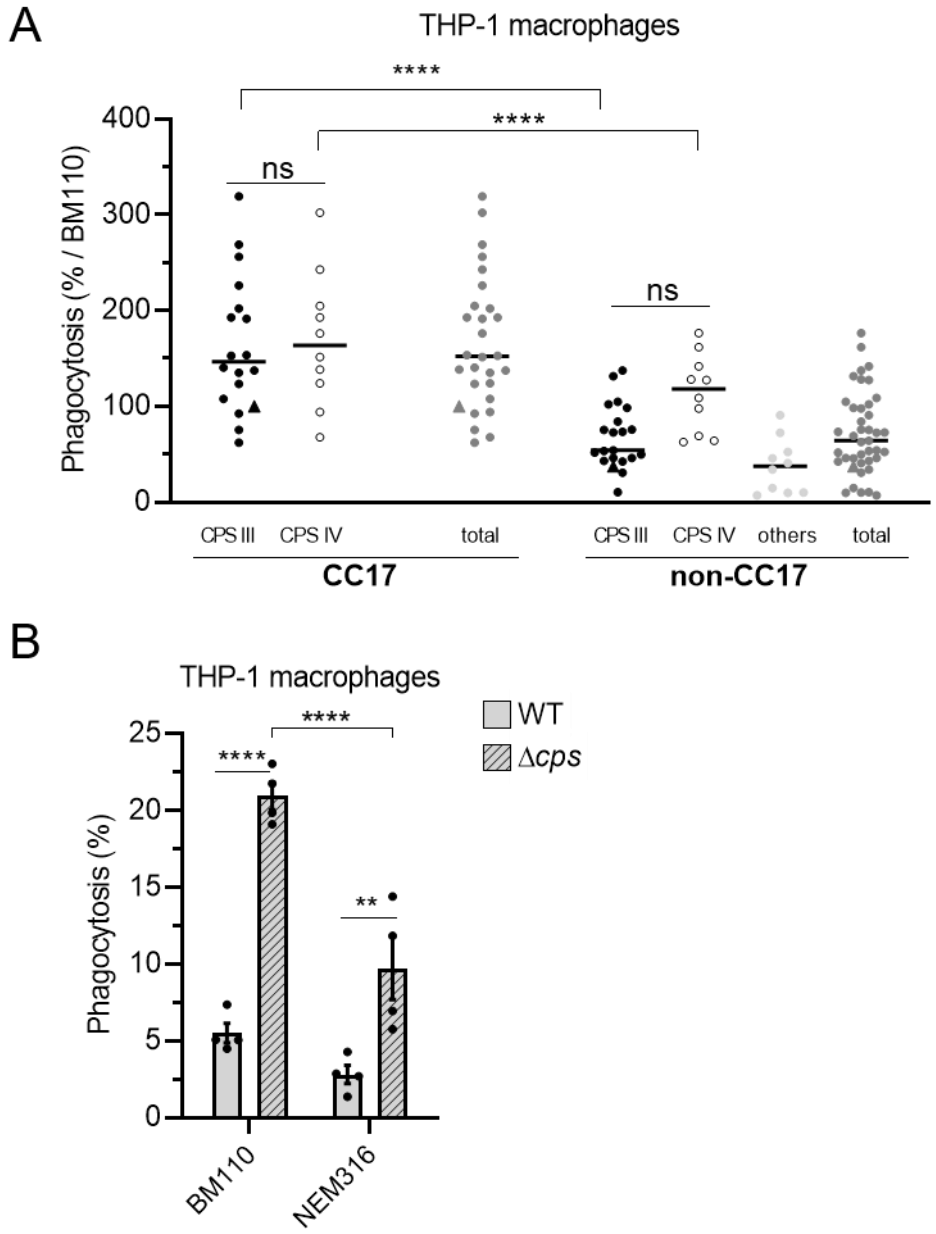

691

692 **Figure 2: GBS capsule is not involved in the hyper phagocytosis of CC17 strains.** (A, B) Phagocytosis
693 level of GBS strains was assessed by CFU count after infection at MOI 10, followed by antibiotic
694 treatment to kill extracellular bacteria. (A) THP-1 macrophages were infected with CC17 and non-CC17
695 GBS clinical isolates from invasive infections, each dot representing a clinical strain. Triangles
696 correspond to BM110 strain (CC17) and NEM316 (non-CC17). Results are shown according to capsular
697 type (CPS III, CPS IV, or other CPSs) and are expressed as the percentage of phagocytosis relative to
698 BM110 strain phagocytosis, with horizontal lines indicating median value. (B) THP-1 macrophages were
699 infected with GBS strains BM1110 and NEM316 and their respective mutant strains impaired for

700 capsule expression (Δ*cps*). Results are expressed as the percentage of phagocytosed bacteria
701 normalized to the initial inoculum.

702 Statistical analysis: data shown are (A) median or (B) mean ± SEM of at least four independent
703 experiments. (A, B) Two-way ANOVA, was performed with ns, non-significant; **, $p < 0.01$; ****, $p <$
704 0.0001.

705

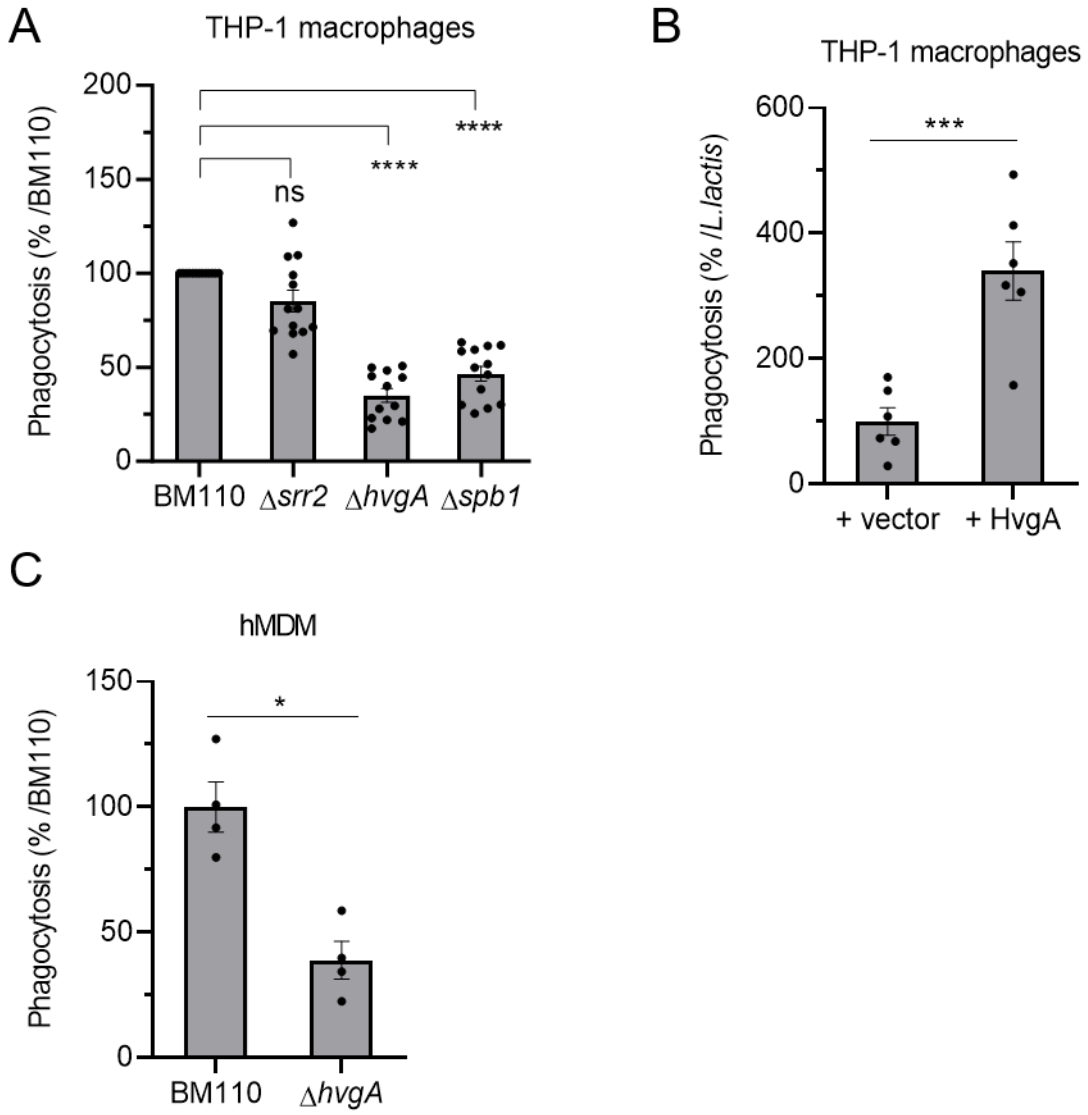

Figure 3: The HvgA surface protein and Spb1 pilus protein are involved in CC17 hyper-phagocytosis. (A, B, C) Phagocytosis level of GBS strains was assessed by CFU count after infection at MOI 10 followed by antibiotic treatment to kill extracellular bacteria using (A, B) THP-1 macrophages (C) hMDM primary cells. (A, C) Macrophages were infected with BM110 and its derivative mutant strains (Δ*srr2*, Δ*hvgA* or Δ*spb1*), or (B) with *Lactococcus lactis* strain carrying an empty vector (+vector) or a vector expressing the HvgA protein (+HvgA). (A, C) Results are expressed as the relative levels to BM110 strain, or (B) to the control *Lactococcus lactis* strain +vector.

Statistical analysis: data shown are mean ± SEM of at least four independent experiments. (A) Kruskall Wallis test with Dunn's multiple comparisons or (B, C) t test, were performed with ns, non-significant; *, $p < 0.05$; ***, $p < 0.001$; ****, $p < 0.0001$.

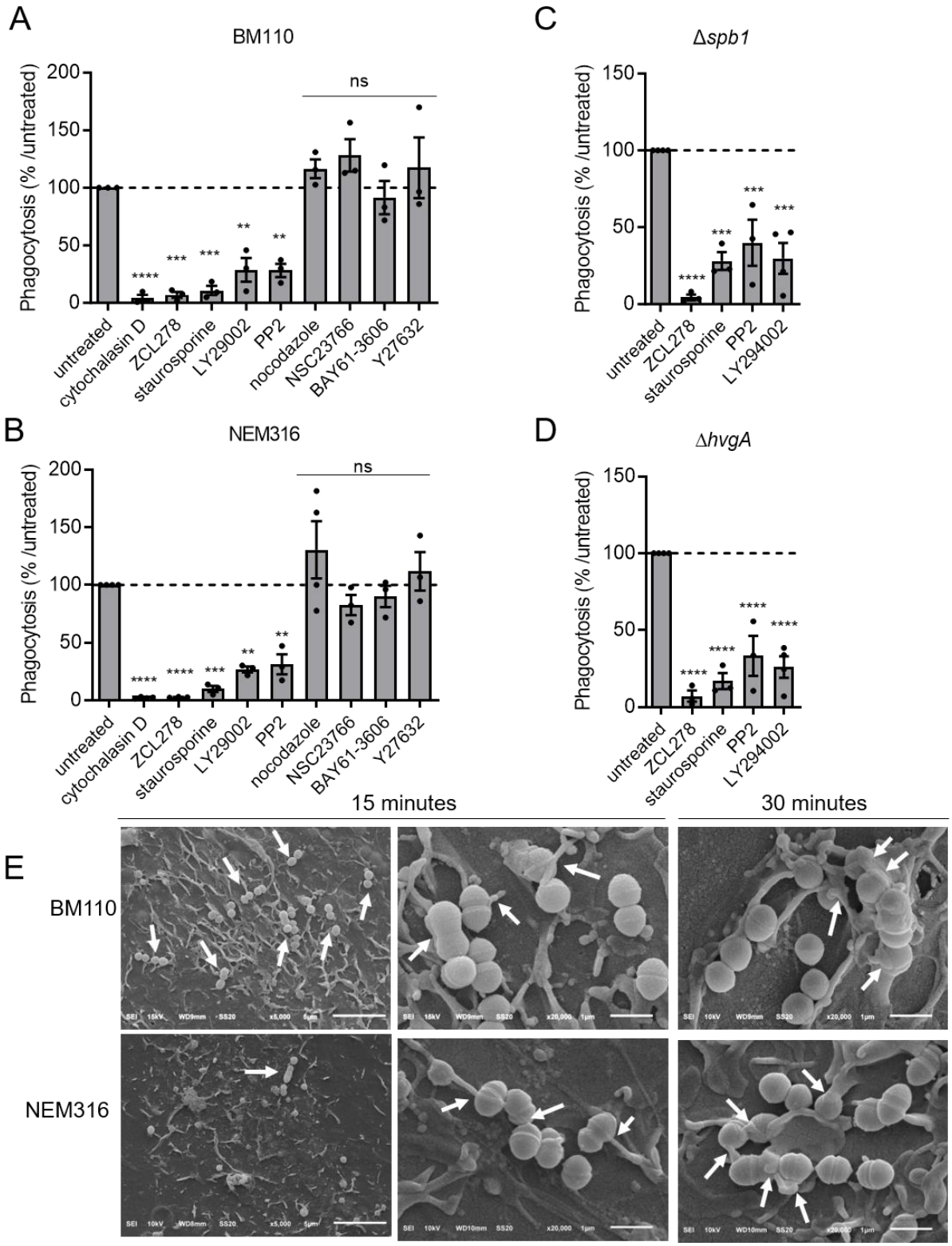

Figure 4: Signal transduction leading to phagocytosis is similar for CC17 and non-CC17 strains. (A, B, C, D) THP-1 macrophages were pre-treated for one-hour prior infection with cytochalasin D, ZCL178, staurosporin, LY29002, PP2, nocodazole, NSC23766, BAY61-3606 or Y27632 to inhibit actin polymerization, CDC42, protein kinase C, PI3kinase, Src kinase, microtubule polymerization, Rac, Syc and Rock, respectively. (A) Phagocytosis level of BM110 (B) NEM316 (C) Δ*spb1* or (D) Δ*hvgA* GBS strains

724 were assessed by CFU count after infection at MOI 10 followed by antibiotic treatment to kill
725 extracellular bacteria. Results are expressed as the relative levels to untreated condition. (E) Scanning
726 electron microscopy (SEM) micrographs of THP-1 macrophages showing (left panel, scale bar 5 µm)
727 bacterial adherence to cell surface and (middle panel and right panels, scale bar 1 µm) bacterial capture
728 by filopodia after 15 min or lamellipodia after30 min of infection.

729 Statistical analysis: data shown are mean ± SEM of at least four independent experiments. One-Way
730 ANOVA with Dunnett multiple comparisons, were performed with ns, non-significant; **, $p < 0.01$; ***,
731 $p < 0.001$, ****, $p < 0.0001$.

732

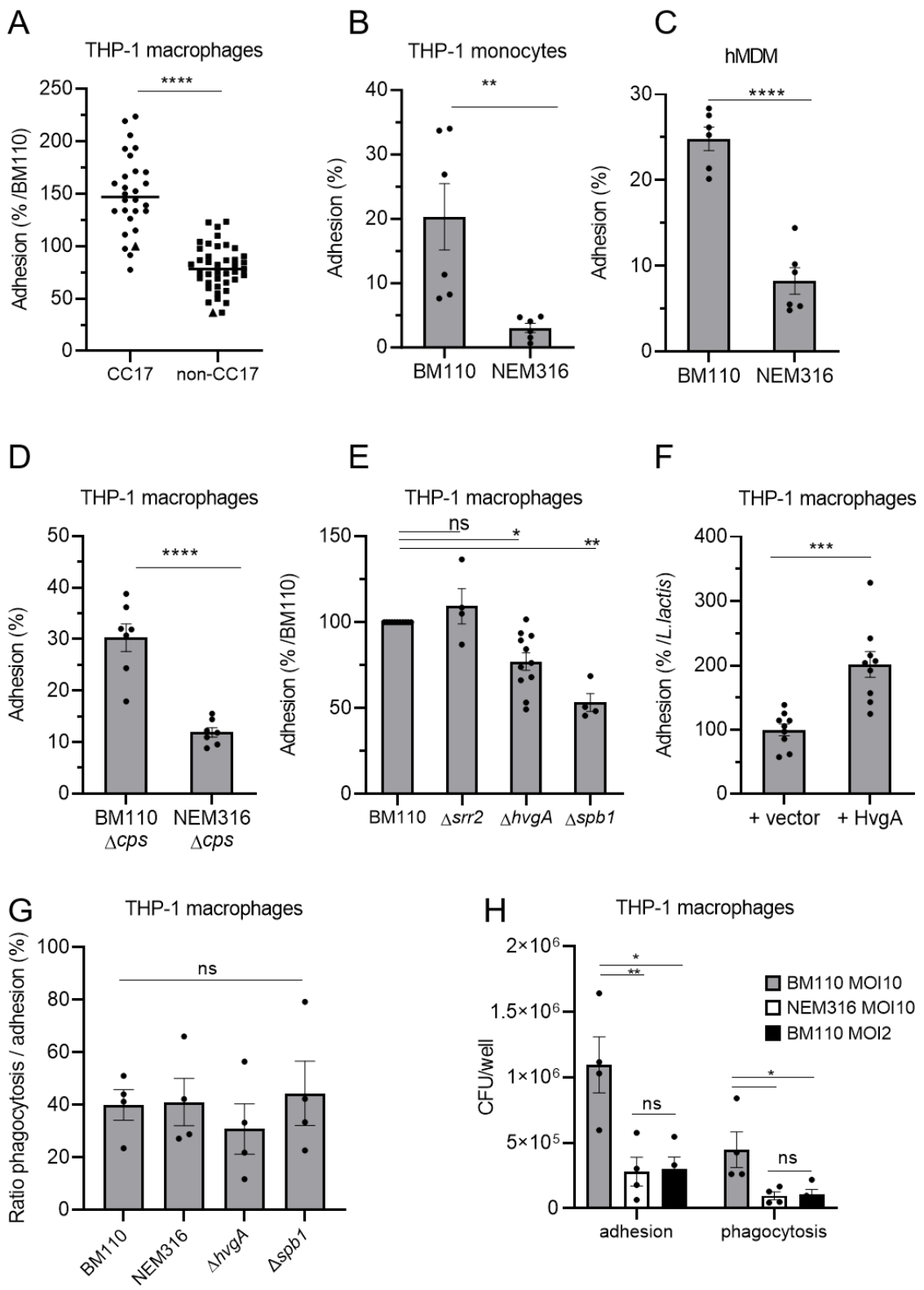

Figure 5: CC17 GBS strains are more adherent to phagocytes than non-CC17 strains. (A, B, C, D, E, F) Adhesion level of GBS strains was assessed by CFU count after infection at MOI 10 at 4°C to avoid bacterial engulfment using (A, D, E, F) THP-1 macrophages (B) THP-1 monocytes (C) hMDM primary cells. (A) Phagocytes were infected with CC17 and non-CC17 GBS clinical isolates from invasive

738 infections, each dot representing a clinical strain. Triangles correspond to BM110 strain (CC17) and
739 NEM316 (non-CC17). Results are expressed as the percentage of adhesion relative to BM110 strain
740 adhesion, with horizontal lines indicating median value. (B, C, D, E, G, H) Phagocytes were infected with
741 GBS strains or (F) with *Lactococcus lactis* strain carrying an empty vector (+vector) or a vector
742 expressing HvgA protein (+HvgA). Results were normalized to (B, C, D) the initial inoculum (E) BM110
743 strain or (F) *L. lactis* control strain (+vector). (G,H) (G) Adhesion and phagocytosis were assessed by
744 CFU count after infection at MOI 10. Results were expressed as the ratio between CFU of phagocytosed
745 bacteria and adherent bacteria. (H) Adhesion and phagocytosis were assessed by CFU count after
746 infection at MOI 10 or 2. Results were normalized to the initial inoculum.

747 Statistical analysis: data shown are mean ± SEM of at least four independent experiments. (A, B, C, D,
748 F) t Test (E) Kruskall Wallis test with Dunn's multiple comparisons or (G, H) One-Way ANOVA with
749 Tukey's multiple comparisons test, were performed with ns, non-significant; *, $p < 0.05$; **, $p < 0.01$;
750 ***, $p < 0.001$; ****, $p < 0.0001$.

751

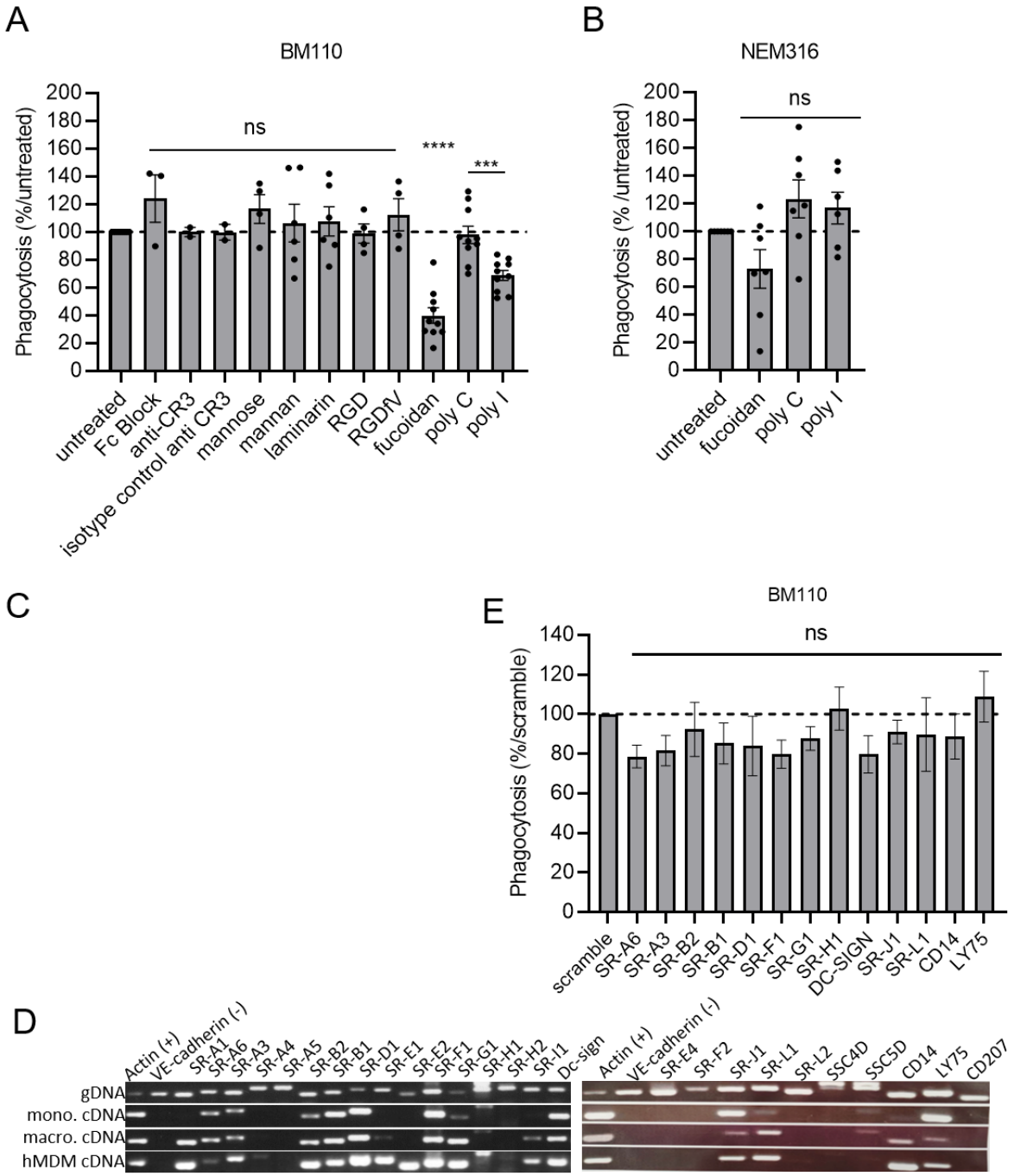

Figure 6: Scavenger receptor inhibitors lead to a decreased phagocytosis level of CC17 GBS in macrophages. (A, B, E) Phagocytosis level in THP-1 macrophages was assessed by CFU count after infection at MOI 10 with (A, E) BM110 or (B) NEM 316 GBS strains followed by 1h antibiotic treatment to kill extracellular bacteria. (A) Macrophages were pre-treated 1h before infection to block FCγ receptors (Fc Block™), complement receptor 3 (CR3 blocking antibody), lectin receptors (mannose, mannan, laminarin), integrins receptors (RGD and RGDfV mimetic peptides), or (A, B) scavenger receptors inhibitors (Fucoidan and poly(I) or inactive analog poly(C). (A, B) Results are expressed as the percentage of phagocytosis relative to the untreated control condition except for poly (I) that was

761 relative to its inactive analogue poly(C). (C) Adhesion level in untreated or fucoidan treated-THP-1
762 macrophages was assessed by CFU count after infection with BM110 and NEM316 at 4°C to avoid
763 bacterial engulfment. Results are expressed as the percentage of phagocytosis relative to the
764 untreated control condition (D) Expression of scavenger receptors genes was assessed by RT-PCR using
765 THP-1 macrophages (macro), THP-1 monocyte (mono) and hMDM (hMDM) cDNA. Actin and VE-
766 cadherin gene expression was used as positive and negative controls of expression, respectively.
767 Genomic DNA (gDNA) was used to validate primers efficiency. (E) Involvement of scavenger receptors
768 on BM110 phagocytosis was assessed by silencing scavenger receptors expression by si-RNA. Results
769 are expressed as the percentage of phagocytosis relative to the scramble control condition.

770 Statistical analysis: data shown are mean ± SEM of at least four independent experiments. (A, B, E)
771 Kruskall Wallis test with Dunn's multiple comparisons or (C) t test were performed, with ns, non-
772 significant; **, $p < 0.01$; ***, $p < 0.001$; ****, $p < 0.0001$.

773

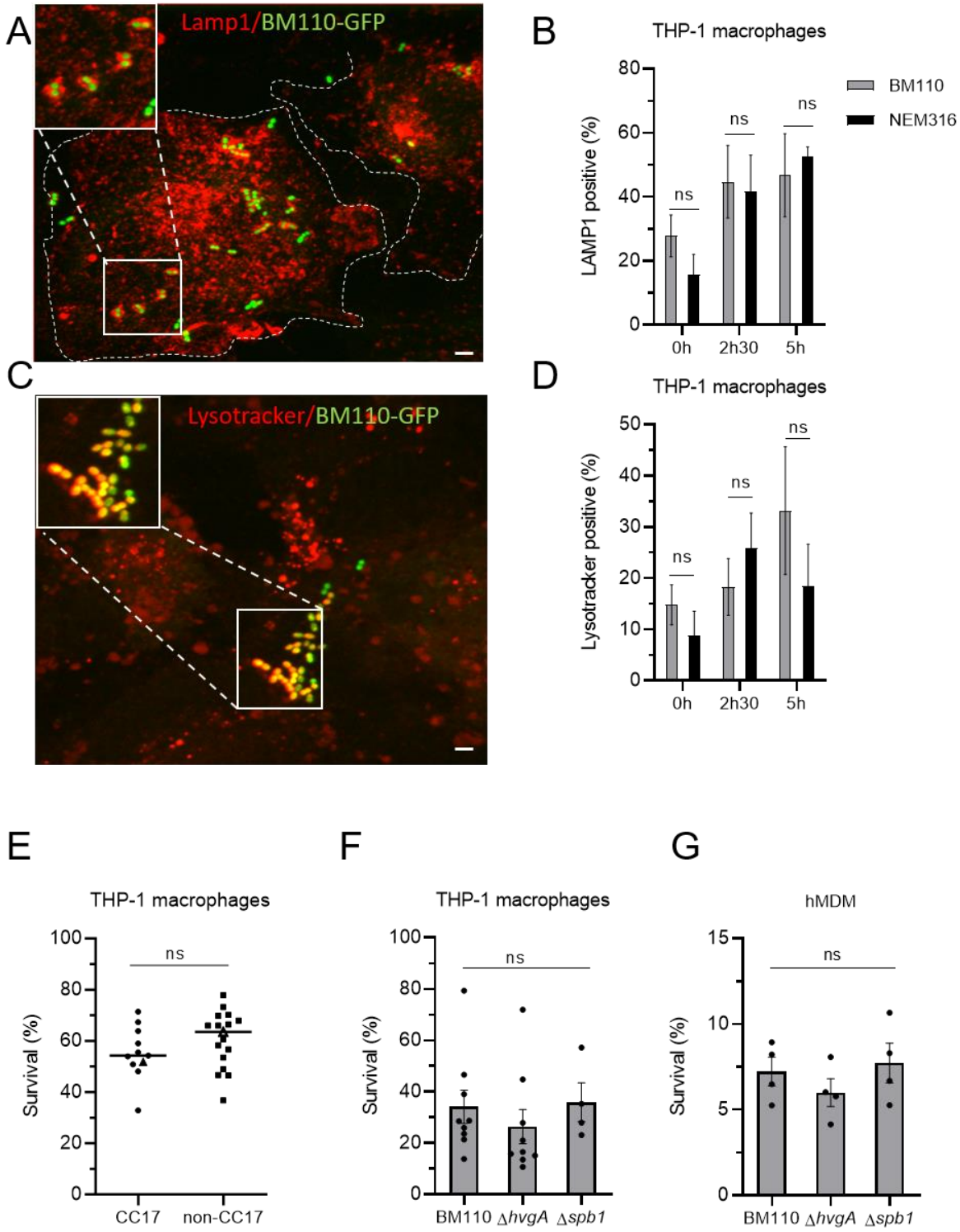

774

775 **Figure 7: CC17 and non-CC17 GBS strains exhibit similar intracellular fate.** (A, B, C, D) Intracellular fate
776 of BM110 and NEM316 strains was followed by microscopy in THP-1 macrophages. (A, C)
777 Representative confocal microscopy images of THP-1 macrophages infected with BM110-GFP (green)
778 and labelled with (A) anti-LAMP1 antibody (red) or (C) Lysotracker® (red). Boxed areas correspond to
779 magnification of insets. Dotted lines indicate cell perimeters. Scale bar: 5 µm. (B, D) Quantification of
780 BM110-GFP and NEM316-GFP associated with (B) LAMP1 or (D) Lysotracker® was performed at 0, 2h30

781 or 5h post-phagocytosis. Results are expressed as the percentage of bacteria positive for (B) LAMP1 or
782 (D) Lysotracker® staining. (E, F, G) Percentage of bacterial survival was assessed by CFU count 2h30
783 after phagocytosis in (E, F) THP-1 macrophage or (G) hMDM. (E) Macrophages were infected with CC17
784 and non-CC17 GBS clinical isolates from invasive infections, each dot representing a clinical strain. For
785 each strain, results are expressed as the percentage of survival relative to corresponding the
786 corresponding level of phagocytosis, with horizontal lines indicating median value. Triangles
787 correspond to BM110 strain (CC17) and NEM316 (non-CC17) (F, G) THP-1 macrophages were infected
788 with the BM110 strain and its derivative mutant strains (Δ*hvgA* or Δ*spb1*). Results are expressed as the
789 percentage of viable intracellular bacteria normalized to the initial intracellular load (phagocytosis).

790 Statistical analysis: data shown are mean ± SEM of at least four independent experiments. (B, D) Two-
791 way ANOVA with Tuckey multiple comparison, (E) t Test or (F) Kruskall Wallis test with Dunn's multiple
792 comparisons or (G) One-Way ANOVA tests were performed with ns, non-significant.

793

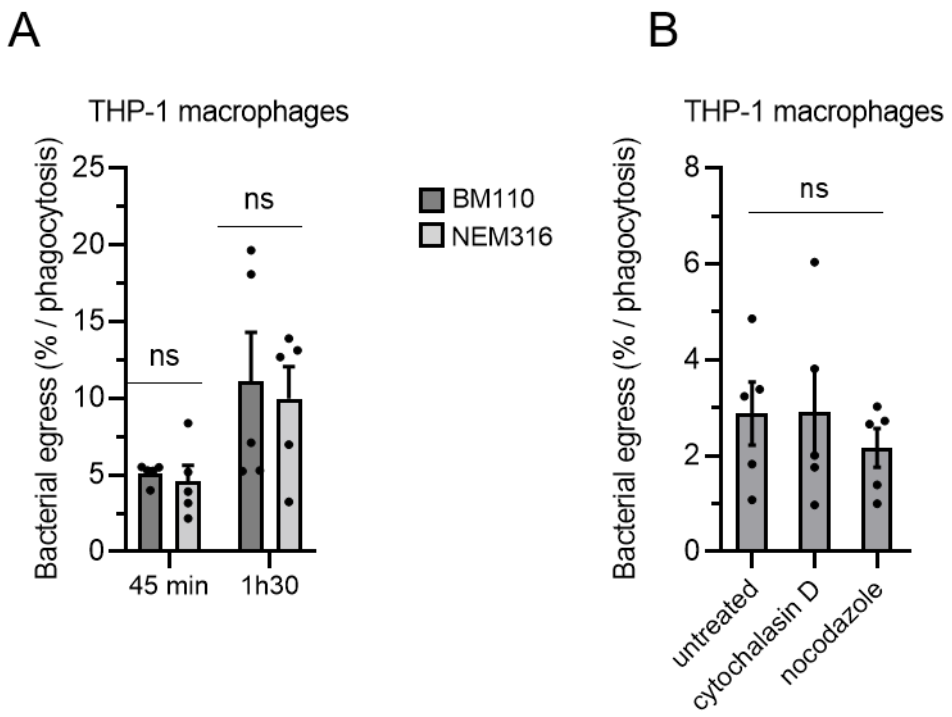

Fig 8: GBS strains can escape macrophages independently of actin and microtubules. (A, B) THP-1 were infected with GBS strains at MOI 10 then treated with antibiotic to kill extracellular bacteria. Bacterial egress was measured by CFU count in cell supernatant devoid of antibiotic after (A) 45 min or 1h30 or (B) 45 min post-antibiotic removal. Results are expressed as the percentage of viable bacteria released in the cell supernatants normalized to the number of phagocytosed bacteria. Bacterial egress was measured for (A) BM110 or NEM316 strains in the absence of treatment or (B) BM110 in the presence of actin (cytochalasin D) or microtubules (nocodazole) depolymerizing agents added after phagocytosis.

Statistical analysis: data shown are mean ± SEM of at least four independent experiments. (A) Two-way ANOVA with Dunnett's multiple comparison (B) one-Way ANOVA with Dunnett's multiple comparisons tests were performed with ns, non-significant.